

# Protease responsive nanoprobes with tethered fluorogenic peptidyl 3-arylcoumarin substrates†

Katharina Welsch,<sup>ab</sup> Jakob Grilj,<sup>c</sup> Eric Vauthey,<sup>c</sup> Jonathan W. Aylott<sup>\*b</sup> and Weng C. Chan<sup>\*a</sup>

Received (in Cambridge, UK) 23rd September 2008, Accepted 13th November 2008

First published as an Advance Article on the web 8th December 2008

DOI: 10.1039/b816637d

Protease responsive nanosensors were obtained by the attachment of unique green fluorescent bifunctional 3-arylcoumarin-derived fluorogenic substrates to poly(acrylamide-co-N-(3-aminopropyl)-methacrylamide) nanoparticles, in which proteolysis results in substantial signal amplification.

Fluorescence bio-imaging has become an indispensable tool for monitoring molecular changes in the intracellular environment. A plethora of ‘smart’ optical devices including fluorogenic substrates,<sup>1</sup> quantum dots,<sup>2,3</sup> near-infrared fluorescence optical probes<sup>4</sup> and optical nanosensors<sup>5</sup> have been developed to provide non-invasive interrogation of enzymatic activity and concentration changes of analytes such as H<sup>+</sup>, Ca<sup>2+</sup> and O<sub>2</sub>. One of the major challenges faced by researchers undertaking cellular studies is the accurate and rapid detection of proteolytic processes *in vivo*.<sup>6</sup> This is important since protease activities are stringently controlled, and their dysregulation commonly results in many disease conditions.<sup>7</sup>

By combining the advantages of fluorogenic substrates and those of optical nanosensors, we have designed a modular tool capable of rapidly and accurately monitoring protease activity. Here we report the synthesis and *in vitro* validation of our so-called ‘protease responsive nanoprobe’ (PRN), which consists of a bifunctional fluorophore attached to both a nanoparticle and a protease specific peptide substrate (Fig. 1). Notably, the fluorogenic moiety is of low molecular weight, displays optimized fluorescence properties and is covalently tethered to the sensor matrix. Compared to non-activatable imaging probes, this approach of proteolytic activation of the imaging probe has the advantage that multiple fluorophores can be switched on by a single enzyme and that protease specificity is achieved by the use of different peptide substrates.<sup>4</sup>

In the design of our fluorescent PRN, we rationalized that the fluorogenic moiety should be a bifunctional and relatively non-toxic reagent with a large Stokes shift and a high quantum yield. The nanoparticle itself should be mono-functionalized, which will enable the covalent attachment of the fluorophore, and should consist of a biocompatible polymer matrix. Thus, we considered the hetero-bifunctional 7-aminocoumarin-4-acetic

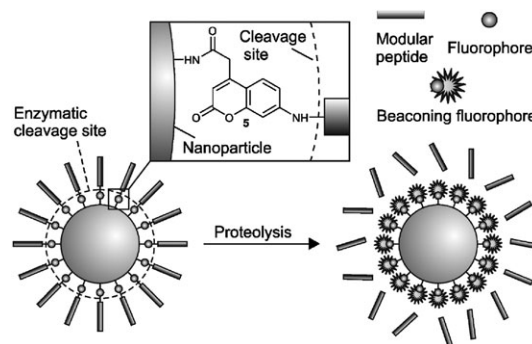
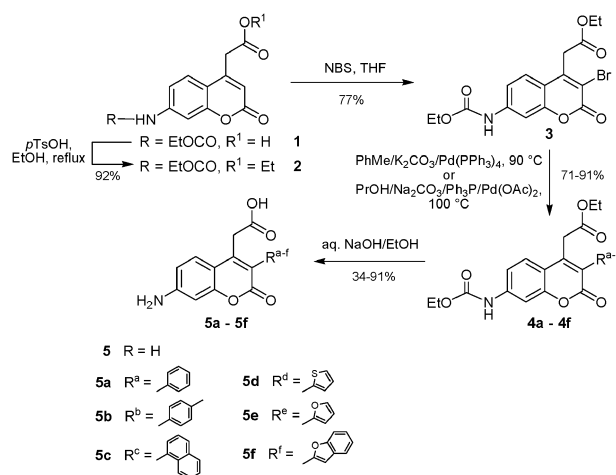


Fig. 1 Model of a protease responsive polymer nanoprobe.

acid (ACA) (**5**) as the fluorophore, which has previously been used to prepare protease substrates.<sup>8</sup> Although **5** has a high quantum yield and large Stokes shift, it shows emission maximum in the blue region making it less ideal for general applications; especially as intracellular probes where the resulting autofluorescence of cells and proteins could be problematic.

With the view to shifting both the absorption and emission maximum of **5** to longer wavelengths, we installed (hetero)-aryl-substituents at the 3-position which extended the  $\pi$  system of the parent fluorophore. Our synthetic strategy to **5** is based on the Suzuki C–C coupling reaction between a coumarinyl bromide and an aryl boronic acid/ester.<sup>9</sup> Thus, the desired intermediate, ethyl 3-bromo-7-*N*-(carbethoxy)amino-coumarin-4-acetate (**3**) (Scheme 1), was obtained in two steps from **1**. We became aware that protection of the 4-carboxymethyl group as an ethyl ester was necessary as significant decarboxylation occurred during the bromination and Suzuki reaction steps. Optimized Pd-catalyzed cross-coupling of **3** with a judicious



Scheme 1 Synthesis of new derivatives of **5**.

<sup>a</sup> School of Pharmacy, Centre for Biomolecular Sciences, University of Nottingham, University Park, Nottingham, UK NG7 2RD.

E-mail: weng.chan@nottingham.ac.uk

<sup>b</sup> School of Pharmacy, Boots Science Building, University of Nottingham, University Park, Nottingham, UK NG7 2RD.

E-mail: jon.aylott@nottingham.ac.uk

<sup>c</sup> Département de Chimie-physique, Université de Genève, 30 Quai Ernest Ansermet, Genève 4, Switzerland CH-1211

† Electronic supplementary information (ESI) available: Experimental protocols and products characterization. See DOI: 10.1039/b816637d/



Fig. 2 Fluorescent characteristics of **5** and its derivatives **5a–5f**.

Table 1 Photophysical properties of **5** and its derivatives **5a–5f**

Reagent	$\lambda_{\text{max/ex}}^a$	$\lambda_{\text{em}}^a$	$\log \epsilon^b$	$\Phi_f^{ac}$	$\tau^{ad}/\text{ns}$
<b>5</b>	345	450	4.11	0.99	5.0
<b>5a</b>	355	460	4.33	0.83	3.7
<b>5b</b>	350	460	4.18	0.68	3.5
<b>5c</b>	355	457	4.41	0.75	3.6
<b>5d</b>	360	484	4.47	0.11	0.6
<b>5e</b>	370	490	4.21	0.26	2.9 (0.7)/0.4 (0.3)
<b>5f</b>	380	496	4.32	0.30	3.2 (0.6)/0.4 (0.4)

<sup>a</sup> Measurements carried out in PBS–10% DMSO. <sup>b</sup> Molar extinction coefficient at  $\lambda_{\text{max}}$  ( $\text{L mol}^{-1} \text{cm}^{-1}$ ; EtOH–5% DMSO). <sup>c</sup> Quantum yields. <sup>d</sup> Fluorescence lifetime; the numbers in parentheses represent relative amplitudes.

selection of (hetero)aryl boronic acids, followed by saponification afforded the unique 3-(hetero)aryl-substituted coumarin derivatives **5a–5f**.

Screening of the derivatives **5a–5f** for their spectroscopic properties (Fig. 2 and Table 1) showed that the modification of **5** in the 3-position with heteroaryls (**5d–5f**) resulted in a significant red shift of both the absorption/excitation ( $\lambda_{\text{max/ex}}$ ) and emission ( $\lambda_{\text{em}}$ ) maxima. Compared to **5**, the shift in  $\lambda_{\text{max/ex}}$  and  $\lambda_{\text{em}}$  was found to be 15–35 nm ( $1200\text{--}2670 \text{ cm}^{-1}$ ) and 34–46 nm ( $1560\text{--}2060 \text{ cm}^{-1}$ ), respectively. In contrast, only a minor shift of  $\lambda_{\text{max/ex}}$  and  $\lambda_{\text{em}}$  was observed for the phenyl, tolyl and naphthyl derivatives. Interestingly, changing the substituent at the 3-position resulted in a general decrease in quantum yields and lifetimes, especially when heteroaryls were incorporated into the ACA scaffold. Similar results have been reported by Bäuerle and co-workers with coumarin.<sup>9</sup> The presence of a new deactivation pathway shows up as a shortening of the fluorescence lifetime for **5d–5f**. The bi-exponential decay for **5e** and **5f** suggests the existence of two different structural forms: one where this new deactivation pathway is operative (hence the shorter  $\tau$ ) and the other where it is inactive (long  $\tau$ ).

From the newly synthesized ACA derivatives, the green fluorophores **5d–5f** were identified as ‘hits’ due to their highly favourable  $\lambda_{\text{max/ex}}$  and  $\lambda_{\text{em}}$ . In fact, compared to the fluorescein dyes ( $\lambda_{\text{max/ex}} = 490 \text{ nm}$ ,  $\lambda_{\text{em}} = 514 \text{ nm}$ ), their Stokes shifts (116–124 nm;  $6150\text{--}7120 \text{ cm}^{-1}$  versus 24 nm;  $950 \text{ cm}^{-1}$  for fluorescein) are particularly noteworthy. Further comparative investigations were then carried out with **5e** because of its ease of synthesis and higher quantum yield when compared to **5d**.

Employing subtilisin as the model protease, an efficient enzyme widely used for studying enzyme–substrate interactions, we proceeded to synthesize the fluorogenic substrates **6**, **6a** and **6e** (Fig. 3). The commercially available Z-Gly-Gly-Leu-AMC (**7**)

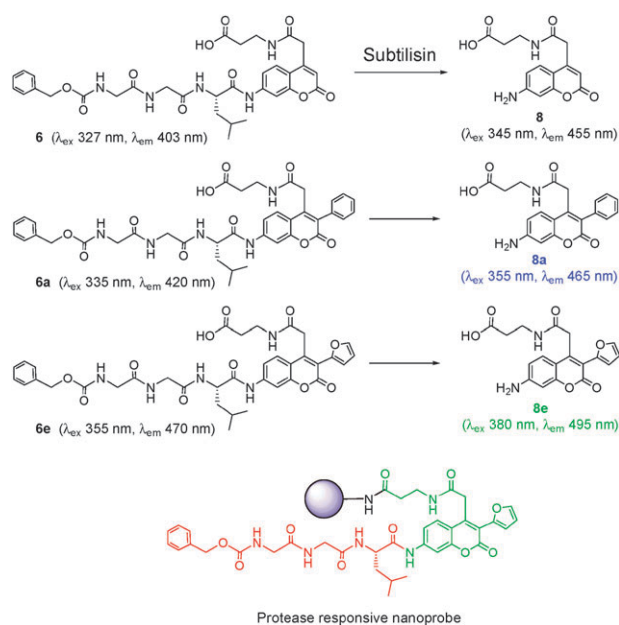


Fig. 3 Chemical structures of fluorogenic probes and nanoprobe.

is a known fluorogenic substrate for subtilisin<sup>10</sup> and was used as a standard. In our model substrates, the ACA 4-carboxylic acid functionality is extended by an amide bond to a  $\beta$ -alanine unit, which is exploited both as a spacer and to endow chemical stability. Because of the poor nucleophilicity of the anilino group in **5**, **5a** and **5e**, it was possible to regioselectively react the fluorophores under mild coupling conditions to  $\beta$ -Ala-preloaded Wang resin without previous Fmoc-protection.<sup>11,12</sup> This was followed by coupling of the C-terminal amino acid residue using HATU/2,4,6-collidine.<sup>8</sup> Assembly of the peptides using a standard Fmoc/*t*Bu solid-phase peptide synthesis method<sup>13</sup> and their subsequent acidolytic release then proceeded smoothly. As anticipated, the prepared fluorogenic substrates displayed blue shifted  $\lambda_{\text{max}}$  and  $\lambda_{\text{em}}$  when compared to the parent fluorophores (see Fig. 3 and 4).

Optimized conditions were then established for the spectrofluorimetric monitoring of the enzymatic cleavage reaction. The specific  $\lambda_{\text{ex}}$  and  $\lambda_{\text{em}}$  were chosen such that the intact substrate showed a minimal absorbance and emission, thus ensuring optimal amplification of the fluorescent signal upon proteolysis. The determined optimized conditions were: **6** ( $\lambda_{\text{ex,opt}} = 380 \text{ nm}$ ,  $\lambda_{\text{em,opt}} = 460 \text{ nm}$ ), **6a** ( $\lambda_{\text{ex,opt}} = 390 \text{ nm}$ ,  $\lambda_{\text{em,opt}} = 470 \text{ nm}$ ), **6e** ( $\lambda_{\text{ex,opt}} = 430 \text{ nm}$ ,  $\lambda_{\text{em,opt}} = 510 \text{ nm}$ ). At these stringently optimized conditions, we observed an approximately 10-fold decrease in the relative fluorescence ( $F_{\text{rel}}$ ) for the ACA(furyl)-based compounds compared to the ACA and ACA(phenyl) derivatives (see Fig. S2 and S3, and

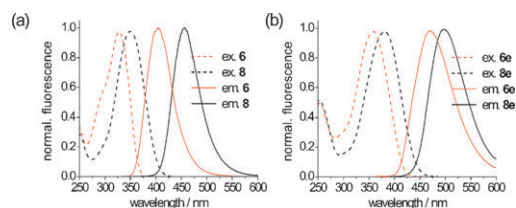


Fig. 4 Normalized excitation (ex., dashed line) and emission spectra (em., solid line) of (a) **6** and **8** and (b) **6e** and **8e** in Tris–HCl buffer.

**Table 2** Kinetic parameters for subtilisin specific fluoroprobes **6**, **6a** and **6e**. Kinetic constants for the AMC standard **7** were taken from ref. 10

Fluoroprobes	$K_M/\text{mM}$	$k_{\text{cat}}/\text{s}^{-1}$	$k_{\text{cat}}/K_M/\text{M}^{-1} \text{s}^{-1}$
<b>6</b>	$0.136 \pm 0.021$	$0.087 \pm 0.005$	$650 \pm 62$
<b>6a</b>	$0.241 \pm 0.037$	$0.086 \pm 0.011$	$359 \pm 10$
<b>6e</b>	$0.263 \pm 0.014$	$0.189 \pm 0.005$	$720 \pm 19$
<b>7</b>	0.740	0.65	880

Table S1, ESI†). However, this decrease in  $F_{\text{rel}}$  is accompanied by significant bathochromic shifts of the excitation and emission maxima as well as an extended Stokes shift, which aids utility of the fluorogenic substrate.

To determine if the introduction of 3-(hetero)aryl-substituents in the ACA structure has an effect on the enzyme–substrate interaction, we carried out enzyme kinetic measurements (Table 2). Compared to the AMC-based substrate **7**,<sup>10</sup> the three ACA substrates are characterized by lower  $K_M$  and  $k_{\text{cat}}$  values. However, among the ACA substrates, **6e** stands out due to a higher  $k_{\text{cat}}$  value and a  $k_{\text{cat}}/K_M$  value that is similar to **7**. These findings together with the feature of having red shifted  $\lambda_{\text{max}}$  and  $\lambda_{\text{ex}}$  highlight the significant utility of our green fluorophore **5e** and its corresponding fluorogenic substrate **6e** for bio-imaging.

To obtain the PRNs, the fluorogenic peptides **6** and **6e** were tethered to amine-functionalized nanoparticles using a standard DIC/HOAt coupling procedure. The nanoparticles derived from acrylamide and *N*-(3-aminopropyl)methacrylamide were prepared *via* an inverse microemulsion polymerization process, which is known to produce nm-sized particles with a narrow size distribution.<sup>14</sup> Characterization by dynamic light scattering (DLS) showed that the nanoparticles were on average approximately 47 nm in diameter (Fig. 5a).

Proof of principle for the concept of PRN was indeed confirmed by a significant increase in fluorescence when the nanoprobe was incubated with subtilisin at 37 °C in Tris–HCl buffer (pH = 8.20) (Fig. 5b). The enzyme reaction slowed after 10 minutes, indicating a fast initial protease response (Fig. 5c). In fact, after 10 minutes, *ca.* 80-fold rise in the fluorescence signal was observed when subtilisin was present at 10  $\mu\text{M}$ . A linear relationship between the initial velocity of nanoparticle-bound **6** and **6e** and subtilisin concentration was observed up to a measured enzyme concentration of 10  $\mu\text{M}$  (Fig. 5d). With initial rates three times as high, PRN comprising **6e** are better enzyme substrates than **6**-derived PRN. These findings are in agreement with our initial enzyme kinetic results outlined in Table 2. Control experiments revealed that no significant change in the fluorescence was observed in the absence of subtilisin or in the presence of chymotrypsin. The concept presented here is modular and hence can easily be extended to other endopeptidases by choosing the appropriate substrates (*e.g.*, see Fig. S4, ESI†).

In conclusion, using rational design principles we have synthesized a new family of fluorescence-based PRNs for the efficient detection of protease activity. These devices consist of a nanoparticle that is covalently attached to fluorogenic peptide substrates comprising spectrofluorimetrically improved bifunctionalized 3-arylcoumarin (**5e**). These customized and

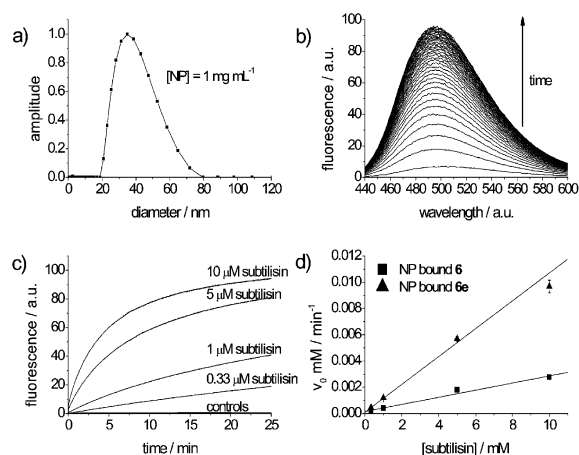


**Fig. 5** (a) DLS of polyacrylamide nanoparticles (NPs); (b) subtilisin mediated cleavage reaction of NP-bound **6e** ( $\lambda_{\text{ex}} = 430 \text{ nm}$ ); (c) enzyme kinetic of NP-bound **6e** at different subtilisin concentrations; (d) initial velocity ( $v_0$ ) versus subtilisin concentration of NP-bound **6** and **6e**.

tunable PRN should find application in diagnostics and high-throughput screening of protease inhibitors. We are currently determining the general utility of different configurations of bio-imaging agents based on our new bifunctional green fluorescent coumarin dye, especially in a cellular and *in vivo* context.

KW would like to acknowledge Engineering & Physical Sciences Research Council and Royal Society of Chemistry, UK for the funding of an analytical science studentship.

## Notes and references

- 1 A. Baruch, D. A. Jeffery and M. Bogoy, *Trends Cell Biol.*, 2004, **14**, 29.
- 2 I. L. Medintz, A. R. Clapp, F. M. Brunel, T. Tiefenbrunn, H. T. Uyeda, E. L. Chang, J. R. Deschamps, P. E. Dawson and H. Mattoussi, *Nat. Mater.*, 2006, **5**, 581.
- 3 M. Zhou and I. Ghosh, *Pept. Sci.*, 2007, **88**, 325.
- 4 M. Funovics, R. Weissleder and C. H. Tung, *Anal. Bioanal. Chem.*, 2003, **377**, 956.
- 5 J. W. Aylott, *Analyst*, 2003, **128**, 309.
- 6 A. Watzke, G. Kosec, M. Kindermann, V. Jeske, H. P. Nestler, V. Turk, B. Turk and K. U. Wendt, *Angew. Chem., Int. Ed.*, 2008, **47**, 406.
- 7 B. Turk, *Nat. Rev. Drug Discovery*, 2006, **5**, 785.
- 8 (a) D. J. Maley, F. Leonetti, J. Backes, D. S. Dauber, J. L. Harris, C. S. Craik and J. A. Ellman, *J. Org. Chem.*, 2002, **67**, 910; (b) J. L. Harris, B. J. Backes, F. Leonetti, S. Mahrus, J. A. Ellman and C. S. Craik, *Proc. Natl. Acad. Sci. U. S. A.*, 2000, **97**, 7754.
- 9 M. S. Schiedel, C. A. Briehn and P. Bäuerle, *Angew. Chem., Int. Ed.*, 2001, **40**, 4677.
- 10 Y. Kanaoka, T. Takahashi, H. Nakayama and K. Tanizawa, *Chem. Pharm. Bull.*, 1985, **33**, 1721.
- 11 J. Deere, G. McConnell, A. Lalaouni, B. A. Maltman, S. L. Flitsch and P. J. Halling, *Adv. Synth. Catal.*, 2007, **349**, 1321.
- 12 Q. Zhu, D. B. Li, M. Uttamchandani and S. Q. Yao, *Bioorg. Med. Chem. Lett.*, 2003, **13**, 1033.
- 13 *Fmoc Solid Phase Peptide Synthesis: A Practical Approach*, ed. W. C. Chan and P. D. White, Oxford University Press, Oxford, 2000.
- 14 *Surfactants and Polymers in Aqueous Solution*, ed. K. Holmberg, B. Jönsson, B. Kronberg and B. Lindman, John Wiley & Sons, Chichester, 2003.